Defence Science Journal, Vol. 62, No. 2, March 2012, pp. 132-136, DOI: 10.14429/dsj.62.1144

SVD-based Method for Radio Frequency Interference Suppression Applied to SAR

Yu Chunrui, Zhang Yongsheng, Dong Zhen, and Liang Diannong

National University of Defense Technology, Changsha, China
E-mail: ycrzxc@163.com

ABSTRACT

Synthetic aperture radar (SAR) is a special type of active microwave sensor, which has got a wide range of applications in remote sensing. However, the performance of SAR systems may be affected by radio frequency interference (RFI) in several geographic regions. A novel singular value decomposition method is proposed for radio frequency interference suppression applied to SAR. This method decomposes the singular vectors of the received signal with RFI into interference subspace and signal subspace. The orthogonality of the two subspaces is used to suppress the RFI. The point-target simulation is used to show the working principle of the proposed algorithm. The experimental results based on SAR real data are also shown to verify the proposed algorithm.

Keywords: Synthetic aperture radar, radio frequency interference suppression, singular value decomposition

1. INTRODUCTION

Remote sensing using microwave sensors has developed much over the last decades. Synthetic aperture radar (SAR) is a special type of active microwave sensor. With the ability of all-day and all-climate observation, SAR has got a wide range of applications and plays an important role in earth observation, environment monitor, disaster predication and military reconnaissance fields. However, some studies indicated that the SAR systems are susceptible to radio frequency interference (RFI) in several geographic regions.

Radio frequency interference is a serious problem for SAR systems especially operating in the low-frequency band, such as the L-band and the VHF/UHF-band. Because the spectrum is widely used by other services, RFI from ground radars and radio communications has been observed in SAR image. Take the L-band SAR JERS-1 for example, according to the statistical evaluation, 27 per cent of the processed images are found to be degraded by these interference signals[1].

Radio frequency interference signals may seriously degrade the SAR image quality, causes significant reduction in image contrast, and introduces image artifacts. Strong interference appears as bright wide stripes in the range direction, superimposed upon the SAR image. The effects of weaker RFI on the amplitude image are in most cases not obvious, however, it is important to note that the influence on the interferometric phase and coherence can be much stronger than the degradation[2,3].

To obtain maximal quality image products, it is desirable to remove the RFI signal prior to image synthesis. Singular value decomposition (SVD) plays an important role in signal processing because it can split a measured data matrix into an interference subspace and a signal subspace[4]. In this paper, a SVD-based adaptive filtering method for RFI suppression is proposed, which can be used to deal with interrupted RFI, and has very good compatibility with existing SAR imaging algorithms. First, to model the RFI as a band limited additive white Gaussian noise (AWGN), and then introduces the principle of SVD. Next, the SVD based algorithm for RFI suppression is used to estimate such interference which then is subtracted from the received signals. At last, simulation and experimental results are provided.

2. RFI SUPPRESSION METHOD BASED ON SVD

2.1 Modeling of RFI

Based on the analysis of the characteristics of RFI[2,4,6,7], a general model of the RFI-contaminated received signal can be deduced. SAR transmits and receives a series of pulses during the coherent processing interval. Suppose there are N range samples in each range line of the SAR data, then the received signal $\boldsymbol{x} = \{x_k \mid k = 1, \cdots, N\}$ at each pulse position can be expressed as

$$x_k = s_k + n_k + j_k \tag{1}$$

where the $\boldsymbol{s} = \{s_k\}, \boldsymbol{n} = \{n_k\}, \boldsymbol{j} = \{j_k\}$ denote the interested signal (the 'pure' ground echo), receiver noise, and RFI signal respectively. In the receiver operating bandwidth, n can be modeled as normally distributed random process with zero mean. For a broad range scene, s can be approximates to white noise. For convenience, rewrite as

$$x_k = j_k + w_k \tag{2}$$

where $\boldsymbol{w} = \boldsymbol{s} + \boldsymbol{n}$. According to the analysis above, $\boldsymbol{w} = \{w_k\}$ can be described as AWGN, suppose the mean noise power is σ_w^2.

Because almost exclusively the RFI signals with a very narrow bandwidth compared to the SAR system bandwidth, then the RFI signal in the received signal can be modelled as a complex sinusoid signal. Suppose a received signal contains P

Received 29 July 2011, revised 10 January 2012, online published 13 March 2012

narrowband RFI signals, then j can be written as:

$$j_k = \sum_{p=1}^{P} A_p e^{j(2\pi f_p k + \theta_p)} \tag{3}$$

where A_p, f_p and θ_p denote the amplitudes, frequencies and phases of the complex sinusoid signals.

2.2 Principle of Singular Value Decomposition

Consider the measured data matrix $\boldsymbol{X} \in \mathbb{C}^{m \times n}$, there exist a unitary matrix $\boldsymbol{U} \in \mathbb{C}^{m \times m}$ and a unitary matrix $\boldsymbol{V} \in \mathbb{C}^{n \times n}$,

$$\boldsymbol{X} = \boldsymbol{U} \Sigma \boldsymbol{V}^H = \sum_{i=1}^{r} \sigma_i u_i v_i^H \tag{4}$$

where $(\bullet)^H$ denotes the Hermitian transpose, and

$$\Sigma = \begin{pmatrix} \Sigma_1 & \mathrm{O} \\ \mathrm{O} & \mathrm{O} \end{pmatrix} \tag{5}$$

where $\Sigma_1 = \mathrm{diag}(\sigma_1, \sigma_2, \cdots, \sigma_r)$ is a nonnegative diagonal matrix. These diagonal entries are called the singular values of $\boldsymbol{X}$ and they are arranged in decreasing order with the largest one in the upper left-hand corner. The columns of $\boldsymbol{U}$ and $\boldsymbol{V}$ called left and right singular vectors, respectively[7].

With the characteristic of white noise, the SAR interested signal has similar singular values which are all close to zero in the absence of RFI with high energy. After large RFI are introduced into the SAR system, there will exist several dominant singular values to represent such interferences. In this case, the data matrix $\boldsymbol{X}$ is the superposition of the SAR signal space and noise space and can be partitioned into two subspaces as follows:

$$\boldsymbol{X} = \begin{bmatrix} \boldsymbol{U}_j & \boldsymbol{U}_s \end{bmatrix} \begin{bmatrix} \Sigma_j & \mathrm{O} \\ \mathrm{O} & \Sigma_s \end{bmatrix} \begin{bmatrix} \boldsymbol{V}_j & \boldsymbol{V}_s \end{bmatrix}^H \tag{6}$$

where

$$\Sigma_j = \mathrm{diag}(\sigma_1, \sigma_2, \cdots, \sigma_r) \tag{7}$$

and

$$\Sigma_s = \mathrm{diag}(\sigma_{r+1}, \sigma_{r+2}, \cdots, \sigma_m) \tag{8}$$

with $\sigma_1 \geq \sigma_2 \geq \cdots \geq \sigma_r \geq \cdots \geq \sigma_m > 0$ corresponding to the singular values in the interference subspace and the signal subspace, respectively; $\sigma_1, \cdots, \sigma_r$ are r largest singular values, i.e. dominant singular values. $\boldsymbol{X}_j = \boldsymbol{U}_j \Sigma_j \boldsymbol{V}_j^H$ and $\boldsymbol{X}_s = \boldsymbol{U}_s \Sigma_s \boldsymbol{V}_s^H$ are the interference subspace and the signal subspace, respectively. By subtracting $\boldsymbol{X}_j$ from $\boldsymbol{X}$, we can get the estimated signal matrix with suppressed RFI.

2.3 Steps of SVD-based RFI Suppression Method

The SVD method for RFI suppression proposed in this paper is a pulse-to-pulse based adaptive method. According to the analysis above, especially the model in and the principle of SVD, for the received signal of each range line, the SVD based RFI suppression method consists of the following main steps:

(a) Construct the measured data matrix $\boldsymbol{X}$, which is the basis for the proposed algorithm. Suppose there are range samples in each range line of the SAR data, then the received data vector of the range line can be defined as $\boldsymbol{x} = [x_1, x_2, \cdots x_N]^T$, where $(\bullet)^T$ denotes the transpose, and $x_k \ (k = 1, \cdots N)$ denotes the k^{th} range sample. Generally, the matrix can be constructed by a Hankel matrix

$$\boldsymbol{X} = \begin{bmatrix} x_1 & x_2 & \cdots & x_{N-L+1} \\ x_2 & x_3 & \cdots & x_{N-L} \\ \vdots & \vdots & \ddots & \vdots \\ x_L & x_{L+1} & \cdots & x_N \end{bmatrix} \tag{9}$$

(b) Perform SVD on $\boldsymbol{X}$, sort its singular values as $\sigma_1 \geq \sigma_2 \geq \cdots \geq \sigma_m$, and find the number of dominant singular values $\hat{r}$.

(c) Pick up the dominant singular values and related principal singular vectors to obtain the estimated interference data matrix

$$\hat{\boldsymbol{J}} = U_{\hat{r}} \Sigma_{\hat{r}} V_{\hat{r}}^H \tag{10}$$

(d) Obtain the RFI cleared data matrix by subtracting the estimation of the interference data matrix $\hat{\boldsymbol{J}}$ from the measured data matrix $\boldsymbol{X}$, which is the estimation of the signal-plus-noise data matrix, and has the form

$$\hat{\boldsymbol{W}} = \boldsymbol{X} - \boldsymbol{J} \tag{11}$$

(e) Rearrange the RFI cleared data matrix $\hat{\boldsymbol{W}}$ into a new vector $\hat{\boldsymbol{w}}$, which is the RFI cleared data from $\boldsymbol{x}$;

(f) Repeat the above steps on a pulse-to-pulse basis until all the pulse have been processed.

3. SIMULATION

The point-target simulation, used to verify the algorithm, is shown in this section. The simulated RFI contaminated signal consists of an LFM signal with noise and four RFI signals. The LFM signal has a bandwidth of 60 MHz and its signal-to-noise ratio (SNR) is 10 dB. The RFI signals are complex sinusoidal signals at frequencies –21 MHz, –11 MHz, 11 MHz, and 19 MHz, with the interference-to-signal ratio (ISR) 16 dB, 12 dB, 12 dB and 16 dB, respectively.

The RFI signals in the simulated 'RFI contaminated signal' can be suppressed by the proposed method, we call the result 'RFI removed signal'. Figure 1 compares the signal waveforms and spectra of the ideal signal, RFI contaminated signal, and the RFI removed signal, where the 'ideal signal' is in the absence of RFI, containing just the LFM signal and random Gaussian noise. It is obvious that most of RFI energy has been removed after the RFI suppression, and the waveform and spectrum of the RFI removed signal is close to the ideal case.

Figure 2 shows the results of the range compressed for the ideal signal, RFI contaminated signal, and the RFI removed signal. In the ideal case, it is very easy to detect the target (top graph). However, the presences of RFI signals make it difficult to detect the target (middle graph). The proposed method helps in reducing the sidelobe energy and enhances the target visibility (bottom graph). The result of the RFI removed signal range compressed compares favorably with the ideal case.

4. EXPERIMENT

In this section, the experimental results using real SAR data are shown to demonstrate the performance of the

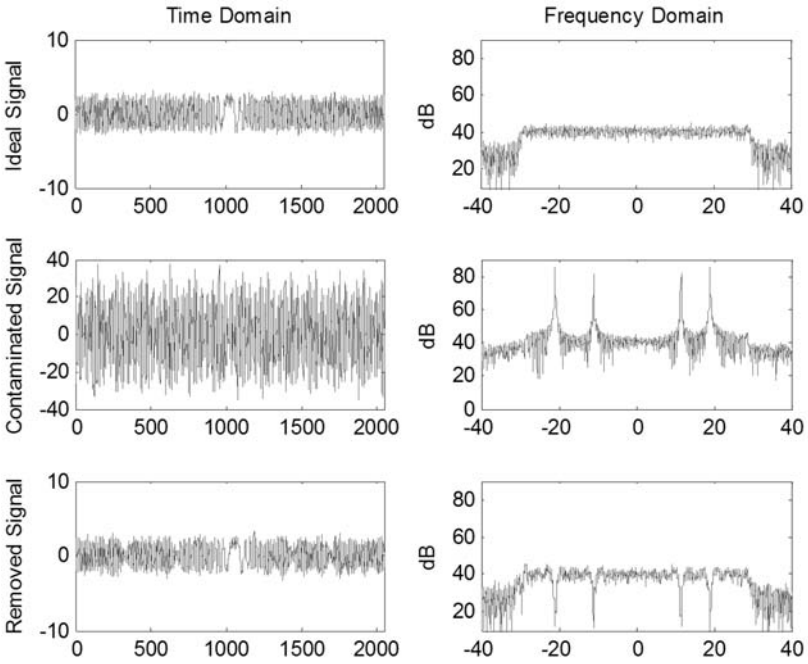

Figure 1. Comparison of signal in time domain and frequency domain.

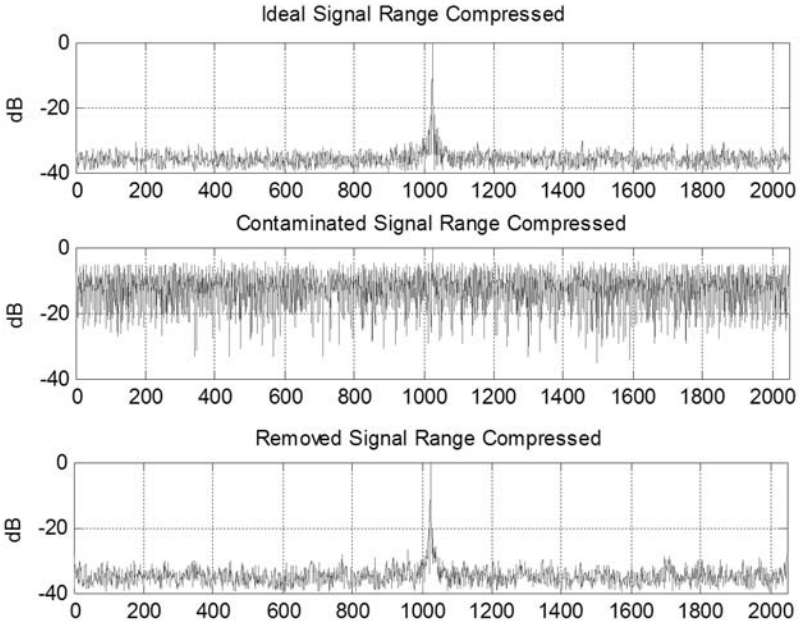

Figure 2. Comparison of results of range compressed.

proposed method.

Because the SAR data with RFI usually in secrecy, we need to obtain the RFI-contaminated experimental data in other way. Based on the signal model and the Eqn (1), the experimental data can be obtained by adding the simulated RFI data to SAR raw data. The procedure of the experiment is shown in Fig. 3. First, read the RADARSAT-1 SAR raw data[8], this data with little RFI, consists of the ground echo and the receiver noise. On the other hand, simulate the RFI data, which consists of four complex sinusoidal signals with random phases and amplitudes. Then, the RFI-contaminated experimental data can be obtained by the superposition of the SAR raw data and the RFI data. To show the effects of the RFI on the SAR image, the RFI just superposed on the last quarter range lines. At last, perform RFI suppression on the experimental data via the proposed method.

The SAR images obtained from different datum above are compared in Fig. 4. Figure 4(a) depicts the SAR image of the raw data (i.e., the ground echo data), showing an area in the vicinity of Vancouver, Canada. In this image, the range dimension is across and along track dimension is up. The scene includes the ships in english bay in the upper left corner of the image, especially. Figure 4(b) shows the image of the RFI-contaminated experimental data, from which it can be noted that RFI appear as bright wide stripes in the range direction, covering the illuminated area, especially the ships in the upper left corner of the image. Because the RFI just superpose on the last quarter range lines, the bright stripes just distributed in the upper region of the image, correspondingly. Figure 4(c) shows the RFI-removed SAR image from the RFI-removed data, which is obtained using the proposed method. Compared with the RFI-contaminated SAR image in Fig. 4(b), the RFI-removed SAR image shows remarkable improvement. The target's visibility is greatly enhanced in the upper region, and the clear bright stripes had disappeared. We can clearly see the ships in the English bay which are very hard to detect in Fig. 2(b). Through the comparison of the images in Fig. 4, it is clearly that the RFI has

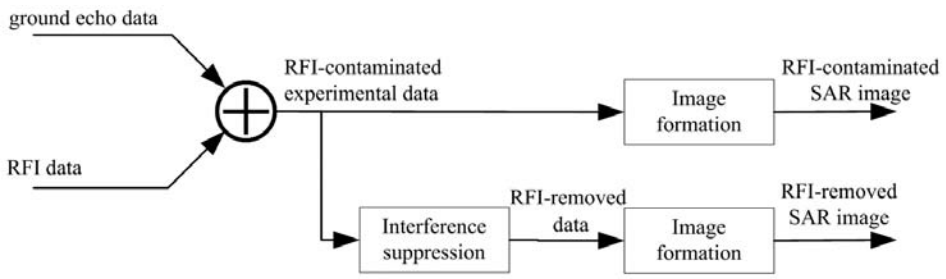

Figure 3. Block diagram of the procedures of the experiment.

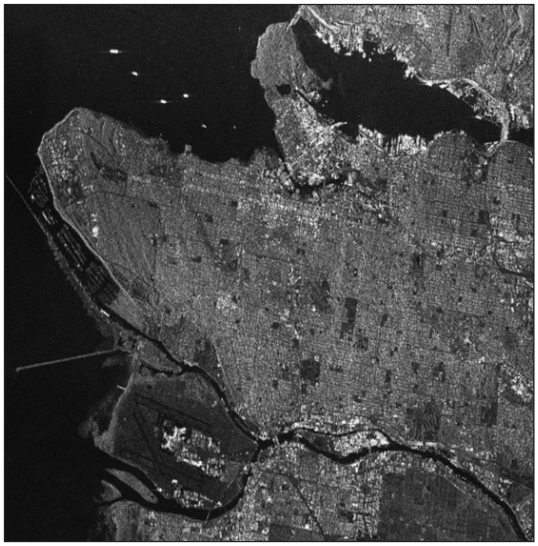

(a)

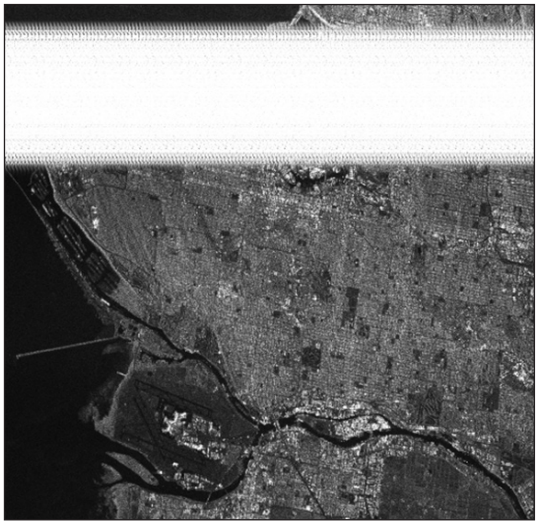

(b)

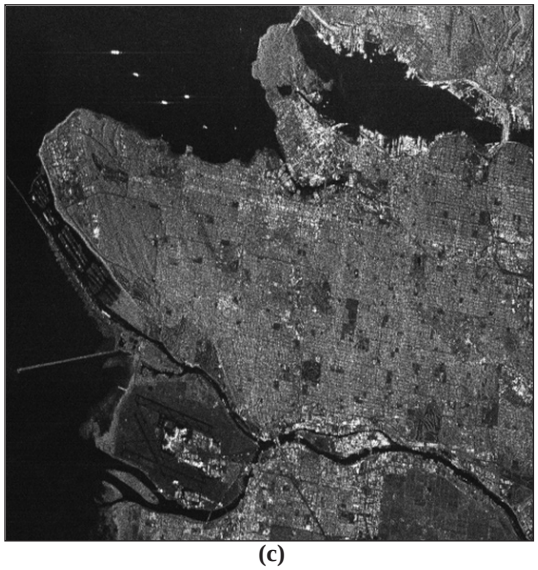

(c)

Figure 4. Comparison of SAR images via different datum: (a) SAR raw data, (b) RFI-contaminated data, and (c) RFI-removed data.

been suppressed effectively and the useful signals have been recovered from the contaminated data efficiently, the proposed method for RFI suppression is low in signal loss and good in interference suppression performance.

5. CONCLUSIONS

Significant radio frequency interference may seriously degrade the SAR image quality. Based on the characteristics of the RFI, This paper shows a simple model for RFI-contaminated SAR data. The SVD-based RFI suppression algorithm is proposed, the key idea of which is to project the RFI contaminated received signal onto the interference subspace and signal-plus-noise subspace. The point-target simulation procedure is described to verify the algorithm's principle. Finally, we have displayed the RFI-contaminated image and compared it with a much improved RFI-removed image. The results show that the proposed method has a good interference suppression performance.

REFERENCES

1. Shimada M. L-band radio interferences observed by the JERS-1SAR and its global distribution. *In* IEEE Geoscience and Remote Sensing Symposium, 2005. pp. 2752-755.
2. Reigber, A. & Ferro-Famil, L. Interference suppression in synthesized SAR images. *IEEE Geosci. Remote Sensing Letters*, 2005, **2**, 45-49.
3. Rosen, P.A.; Hensley, S. & Le, C. RADAR. Observations and mitigation of RFI in ALOS PALSAR SAR data: Implications for the DESDynI mission. *In* IEEE Radar Conference, Rome, Italy, 2008. pp. 1-6.
4. Xu, S.; Bai, S.; Yang, Q. & Kwak, K. Singular value decomposition-based algorithm for suppression of IEEE 802.11 a interference in multiple access TH-UWB systems. *In* ISCIT, 2006. pp. 599-604.
5. Chan, S.M.S. RFI study for the SMAP radar. *In* IEEE Radar Conference, Pasadena, CA, 2009, pp. 1-5.
6. Charles, T.C. Le; Hensley, Scott & Chapin, E. Removal of RFI in wideband radars. International Geoscience and remote sensing Symposium, 1998, Sheraton Seattle, WA, USA, **2**, pp. 2032-034.
7. Zhang, X. Matrix analysis and applications. Tsinghua University Press, Beijing, 2004. pp. 341-400.
8. Ian, G.C. & Wong, F.H. Digital processing of synthetic aperture radar data: Algorithms and implementation. Artech House, Norwood, MA. 2005. pp. 587-88.

Contributors

Mr Yu Chunrui received his MS (Communication Engineering) from National University of Defense Technology (NUDT), Changsha, China in 2007. He is currently pursuing PhD (Information and Communication Engineering) from NUDT. His research interests include : Synthetic aperture radar (SAR) imaging, SAR jamming and anti-jamming, and space-time adaptive processing.

Dr Zhang Yongsheng received his BE and PhD degrees in signal processing from NUDT, in 1999 and 2007, respectively. He is currently a Lecturer in the Institute of Space Electronic and Information technology, NUDT. His research interests include SAR system design, SAR jamming and anti-jamming, and space-time adaptive processing.

Dr Dong Zhen received his BE and PhD (Information and Communication Engineering) from NUDT in 1997 and 2001 respectively. He is currently a researcher in the Institute of Space Electronic and Information technology, NUDT. His research interests include SAR imaging and target detection, SAR jamming and anti-jamming, and radar signal processing.

Mr Liang Diannong graduated from Harbin Institute of Military Engineering, Harbin, China in 1958. He is currently working as a professor in NUDT. He has more than 50 years research experience in the field of adaptive signal processing, radar systems design, SAR imaging and target detection, and radar array processing.